A&A 553, A64 (2013)
DOI: 10.1051/0004-6361/201219644

Astronomy & Astrophysics

CO(6−5) and [C I](2−1) pointed observations of five protoplanetary disks: Warm gas in HD 142527⋆ *(Research Note)*

S. Casassus[1,2], A. Hales[3], I. de Gregorio[3,4], B. Dent[3], A. Belloche[5], R. Güsten[5], F. Ménard[6,7], A. M. Hughes[8], D. Wilner[9], and V. Salinas[1]

[1] Departamento de Astronomía, Universidad de Chile, Chile
e-mail: simon@das.uchile.cl
[2] Observatoire de Paris, LUTH and Université Denis Diderot, Place J. Janssen, 92190 Meudon, France
[3] Joint ALMA Observatory, Alonso de Córdova 3107, Vitacura 763-0355, Santiago, Chile
[4] European Southern Observatory, Alonso de Cordova 3107, Vitacura. Casilla 19001, 19 Santiago, Chile
[5] Max-Planck Institut für Radioastronomie, Auf dem Hügel 69, 53121 Bonn, Germany
[6] UMI-FCA, CNRS/INSU France UMI 3386, and Departamento de Astronomía, Universidad de Chile, Casilla 36-D Santiago, Chile
[7] CNRS/UJF Grenoble 1, UMR 5274, Institut de Planétologie et d'Astrophysique de Grenoble (IPAG), 38041 Grenoble Cedex 9, France
[8] Wesleyan University Department of Astronomy, Van Vleck Observatory, 96 Foss Hill Dr., Middletown, CT 06459, USA
[9] Harvard-Smithsonian Center for Astrophysics, 60 Garden Street, Cambridge, MA 02138, USA

Received 22 May 2012 / Accepted 25 March 2013

ABSTRACT

Context. The molecular gas in protoplanetary disks can be traced with single-dish instruments in low J rotational lines of CO, in systems clear of coincident extended emission. Other rotational lines of CO also sample the gas-phase CO reservoir, albeit with different biases; CO(6−5) traces warmer molecular gas. A rarefied atomic gas could be traced in [C I](2−1), but no C I detections in disks exist.
Aims. Our goals are to identify gas-rich systems that are bright in CO(6−5), for subsequent ALMA observations, and search for C I.
Methods. We follow-up a CO(3−2) survey in protoplanetary disks with APEX/CHAMP+ maps in CO(6−5) 691.4 GHz and [C I](2−1) 809.3 GHz.
Results. We obtain one compact CO(6−5) detection in HD 142 527, three upper limits, and extended CO(6−5) emission in HD 37389. Given the CO(2−1) flux, the CO(6−5) line in HD 142527 would imply a temperature of 19 K if the CO ladder was isothermal, for a common solid angle, which is close to CO freezeout. This low temperature, together with a modulated CO(6−5) line profile, can be explained by a 4″ pointing offset. The C I observations yield upper limits on the mass of rarefied gas phase neutral carbon.
Conclusions. The CO(6−5) detection in HD 142527 adds to the other two southern systems with known CO(6−5) signal (HD 100546 and TW Hya). The CO(6−5)/CO(3−2) flux ratio varies from 2 to 24 among seven sources with bona-fide CO(6−5) detections, and is uncorrelated with spectral type in this sample. The upper limits on CI emission constrain the fraction of carbon in low-density ($<10^3$ cm^{-3}) atomic gas to $<4 \times 10^{-3}$ (3σ).

Key words. protoplanetary disks – stars: emission-line, Be

1. Introduction

Observable signatures of giant planet formation, such as gaps and spirals (Wolf & D'Angelo 2005; Alexander & Armitage 2007) are expected in protoplanetary disks containing residual gas in Keplerian rotation. But mapping the gas in protoplanetary disks is difficult. Most of the gas mass is in cold molecular hydrogen that does not emit any significant radiation (for a summary of the optical/IR diagnostics of gas in disks see Carmona 2010). Sub-mm rotational CO emission is often used as a proxy for the bulk molecular gas. Substantial masses of gas are indeed detected towards young (1−10 Myr) disks (e.g. Dutrey et al. 1996; Dunkin et al. 1997; Thi et al. 2001; Hughes et al. 2008; Öberg et al. 2010), but not in more evolved systems (Zuckerman et al. 1995; Duvert et al. 2000; Dent et al. 2005).

The whole rotational ladder of CO is expected to be optically thick in young disks. The CO(6−5) line stems from warmer gas than the lower-J lines. The temperature-equivalent of the upper level energies are 116 K for CO(6−5), 33 K for CO(3−2). The emergent fluxes in the CO ladder are largely determined by the distribution of temperature in the unit-opacity surfaces; CO(6−5) should be higher above the mid-plane than CO(3−2). However the emergent fluxes, and expected excitation temperatures distributions, depend on the radiative transfer of the CO lines, which has to be solved for a given model disk. Thus comparisons of maps and spectral profiles in CO(6−5) and CO(3−2) yield information on the temperature structure of

⋆ Based on observations carried out with the Atacama Pathfinder Experiment telescope (APEX). APEX is a collaboration between the Max-Planck Institut fr Radioastronomie, the European Southern Observatory, and the Onsala Space Observatory.

Table 1. CHAMP+ observations of five protoplanetary disks.

	t^a	pwv^b	[C I](2−1)		CO(6−5)	
			τ,$T_{sys}{}^c$	$T_{mb}{}^d$	τ,$T_{sys}{}^c$	$T_{mb}{}^d$
HD 142527	40	0.53	0.99, 3497	±2.05	0.88, 1338	1.03 ± 0.22^e
VV Ser	40	0.51	0.97, 4416	±2.65	0.85, 1544	±0.97
rxj 1842.9-35	40	0.48	0.84, 3941	±1.85	0.76, 1465	±0.71
HD 178253	70	0.44	0.80, 4455	±1.45	0.73, 1699	±0.56
HD 37389	50	0.40	0.75, 4475	±1.67	0.68, 1607	±0.64^f

Notes. All values preceded by "±" are the root-mean-square (rms) scatter noise in K, i.e. 1σ, without binning. Practical upper limits on the amplitude of Gaussian lines with a FWHM Δ_v are given by $\approx 2.91\sigma/\sqrt{\Delta_v/\delta_v}$, with 99.7% confidence, and where the channel widths δ_v are 0.068 km s^{-1} in [C I](2−1) and 0.079 km s^{-1} in CO(6−5). $^{(a)}$ Duration of each observation, in mn, including overheads such as time on the reference positions, wobbler and slew times, and load calibrations; $^{(b)}$ radiometer precipitable water vapour column, in mm; $^{(c)}$ atmospheric opacity and system temperature (in K); $^{(d)}$ main-beam temperature T_{mb}, in K, converted from $T_A^\star$ with $T_{mb} = 2.64\ T_A^\star$; $^{(e)}$ amplitude of Gaussian fit, with 1σ error bar. The unbinned rms scatter under the line was 0.79 K. See the text for Gaussian-fit parameters; $^{(f)}$ extended emission in the central horn reaches $T_{mb} \sim 1.4$ K.

the CO gas. Thi et al. (2001) detected CO(6−5) emission towards 8 sources in Taurus-Auriga, in pointed single-dish data[1]. Van Zadelhoff et al. (2001) found CO(6−5) in LkCa 15; in their models the spatial profile of the unit-opacity surfaces for CO(6−5) and CO(3−2) are similar (with heights above the midplane within 10% of each other, their Fig. 6). Qi et al. (2006) reported on CO(6−5) interferometric observations of TW Hya. They model their dataset in terms of the vertical temperature structure and X-ray heating. Recently Panić et al. (2010) found intense CO(6−5) emission from HD 100546 with a spectral profile similar to CO(3−2), and correspondingly similar model radial distributions. The CO(6−5)/CO(3−2) line ratio matches optically thick emission at 60−70 K.

The 7-horn CHAMP+ receiver (Güsten et al. 2008) on the APEX telescope allows the observation of high-J CO lines in southern disks while also sampling the coincident extended emission with its peripheral horns, as in Panić et al. (2010). In addition, CHAMP+ also covers the [C I](2−1) ground-state fine-structure line, which is a measure of the atomic carbon content in disks.

Here we report on a CHAMP+ search for the molecular gas reservoir in 5 disks. These sources are potential targets for the Atacama Large Millimetre Array (ALMA, e.g. Wootten & Thompson 2009), and are currently the subject of detailed observational studies. Section 2 gives details on the observational setup and target selection. Our results are described in Sect. 3; we highlight the detection of CO(6−5) in HD 142527. All other measurements yield upper limits. Sect. 4 concludes.

2. Observations and target selection

Our CO(3−2) survey of 52 pre-main-sequence and main-sequence stars with circumstellar dust excesses resulted in several detections (about 1/3 detection rate, Hales et al. 2013, in prep., COSURVEY hereafter). However, in most cases the contribution from ambient cloud emission or coincident extended emission are ambiguous, so we need to confirm our detection by independent means. We selected a sample of disks for follow-up observations with CHAMP+ in CO(6−5) 691.4 GHz and [C I](2−1) 809.3 GHz. The sample includes both HAeBe stars and T-Tauri stars. CHAMP+ was mounted on the APEX 12 m single dish (Güsten et al. 2006) during our observations, spread around midnight on 01-Aug-2010.

Our sample of disks was extracted from our own and literature CO(3−2) detections, and avoiding sources blocked by ongoing CHAMP+ programmes. The observational setup we chose is very similar to that used by Panić et al. (2010), except that we used symmetric wobbler switching for cancellation of extended emission (as described in Menten et al. 2011), with a 120″ throw both-ways in direction of cross-elevation, at a rate of 1.5 s. The derotator was turned on so that the CHAMP+ 7-horn footprint was kept fixed on the sky. The beam spacing and angular separation between the outer hexagon and the central horn is 19″ (about 2.15 times the beam FWHM in CO(6−5)).

CHAMP+ is a dual-color heterodyne array for simultaneous spectroscopy in the 450 μm and 350 μm atmospheric windows, with beam FWHM of 8.″8 and 7.″7. For each window the FFT spectrometer gives two 1.5 GHz bandwidths, AF01 and AF02, with 8192 channels each, overlapping at the centre frequency, where the signals are redundant. We used AF02, which was less affected by glitches. The spectral resolution is 212 kHz, so slightly greater than the channel width. Antenna temperature ($T_A^\star$) calibration was obtained with a cold load, and converted into main beam temperature (T_{mb}) with an antenna efficiency of η_f/η_S, where the forward beam-efficiency $\eta_f = 0.95$, and $\eta_S = 0.36$ (as obtained from Mars observation in July 2010; efficiency values are available in the MPIFR web pages). The average total time spent per source was ∼1 h. Weather was stable and clear, with a column of precipitable-water-vapour that varied from 0.60 mm (at sunset on 31-Jul-2010) to 0.38 mm (at sunrise on 01-Aug-2010).

3. Results

Table 1 summarises the observations. We obtain one bona-fide spatially unresolved CO(6−5) detection in HD 142527.

3.1. HD 142527

HD142527, at a distance of ∼140 pc, is an F6IIIe star that is considered as a member of the young HAeBe class (Malfait et al. 1998), i.e. a 1.9 $M_\odot$ young star with a disk. HD 142527 has an extremely strong IR excess, $L_{IR}/L_\star = 1.09 \pm 0.04$ (Fukagawa et al. 2010). SMA imaging by Ohashi (2008) shows a circumstellar torus in the continuum, about 1″ in radius, possibly matched by CO(3−2). However recent observations showed

[1] From this sample we selected the most convincing detections, i.e. LkCa 15, GM Aur, V 892 Tau, GG Tau and MWC 480.

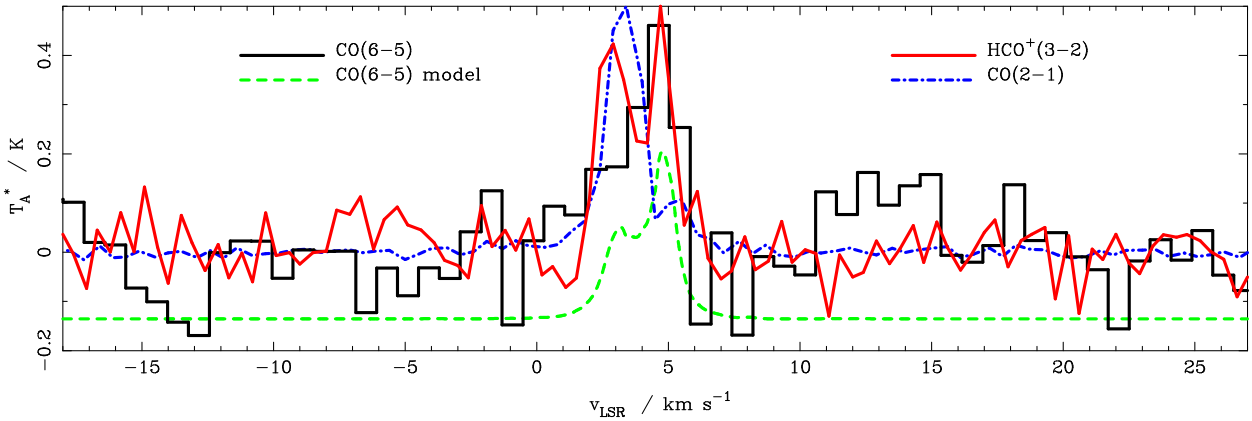

Fig. 1. CHAMP+ observations of HD 142527 in CO(6−5) and comparison spectra. The black histogram shows the CHAMP+ central horn spectrum in CO(6−5), with $T_{\rm A}^{\star}$(K) in y-axis and $v_{\rm lsr}$(km s^{-1}) in x-axis. The blue dot-dashed line and the red solid line are the SMA CO(2−1) and HCO+(3−2) profiles from Öberg et al. (2011), in arbitrary units. A comparison model for CO(6−5) is shown in green dashed lines, in $T_{\rm A}^{\star}$(K), modulated by a pointing offset of 4″ southwards, and offset for clarity.

strong CO(3−2) emission inside the cavity (Casassus et al. 2013).

Fukagawa et al. (2006) reported H and K band coronographic images that reveal an inner hole and an outer arm. This inner cavity is in fact a gap because of the large IR excess, which suggests an inner disk (resolved by van Boekel et al. 2004). The inner cavity has also been resolved in the mid-IR (Fujiwara et al. 2006; Verhoeff et al. 2011); overall the multi-wavelength data is consistent with an inclination angle of ∼20−30 deg.

With CHAMP+ we find CO(6−5) emission in the central horn towards HD 142527, as illustrated in Fig. 1. The lack of signal in the outer horns supports that central horn detection is probably associated to the disk and not with the extended diffuse screen seen in single-dish CO(3−2) (COSURVEY). The CO(6−5) spectrum shown in Fig. 1 has been smoothed by re-binning into 10 channel averages. We also show a comparison model (see below), and the CO(2−1) and HCO+(3−2) spectra from Öberg et al. (2011, interferometric data). There is an intriguing velocity shift of ∼1 km s^{-1} between the two CO lines. Despite careful pointing calibration, it is conceivable that a pointing error could modulate the CO(6−5) profile. The pointing corrections that immediately bracketed HD 142527 were of 3 and 7″. As can be inferred by inspection of Fig. 2 in Öberg et al. (2011), a pointing offset by ∼4″ to the south would sample the red-shifted parts of the disk, and attenuate the blue emission. It is revealing that HCO+(3−2) also displays a markedly different profile, double-peaked as expected and with a centroid intermediate between CO(2−1) and CO(6−5). Since our single-dish CO(3−2) spectrum acquired with APEX shows strong extended emission over $4.5 < v_{\rm lsr}/{\rm km\ s^{-1}} < 6$, it is also likely that CO(2−1) is absorbed in the red (the cloud emission adds to single dish observations, but is filtered from interferometric observations without total power, leaving an absorption in the latter case).

The comparison CO(6−5) model shown in Fig. 1 was obtained with the LIME radiative transfer code (Brinch & Hogerheijde 2010). We assumed fiducial parameter values, as in Casassus et al. (2013, , their supplementary information): an inclination of 20 deg (Verhoeff et al. 2011), a constant CO abundance of 10^{-4} relative to H_2, and an azimuthally-symmetric H_2 number density

$$n_{\rm H2}(r,z) = 1.5\times10^{14}\left(\frac{r}{100\ {\rm AU}}\right)^{-1.5}\exp\left[-\frac{1}{2}\left(\frac{z}{0.1\,r}\right)^2\right]\ {\rm m^{-3}},$$

from 140 to 300 AU, and

$$n_{\rm H2}(r,z) = \zeta\ 1.5\times10^{14}\ \exp\left[-\frac{1}{2}\left(\frac{z}{0.1\,r}\right)^2\right]\ {\rm m^{-3}},$$

from 10 to 140 AU, and zero elsewhere. This model corresponds to a sharp-edged ring in surface density, enclosing a flat and shallow cavity whose depth in surface density is $\zeta = 1/10$ relative to the peak on the ring. The total mass of the model is ∼0.1 $M_\odot$[2]. The temperature profile was $T(r) = 45\ [r/(100\ {\rm AU}]^{-1/2}$ K, with a maximum of 64 K, so reaching moderately higher temperatures than the model for CO(3−2) in Casassus et al. (2013). The predicted spectrum at a distance of 140 pc was then scaled to $T_{\rm A}^{\star}$ units. An approximate match to the observed CO(6−5) profile can be obtained by modulation with a Gaussian representative of an off-centre CHAMP+ pointing.

Since we do not have enough dynamic range to study the CO(6−5) profile in detail, we use a simple Gaussian fit to report basic properties, with a reduced χ^2 of 0.82 for a rms noise of 0.79 K ($T_{\rm mb}$). The FWHM of the line is $\Delta_v = 2.52^{+0.73}_{-0.75}$ km s^{-1}, its centroid is $v_\circ = 4.13 \pm 0.32$ km s^{-1}, and its amplitude in $T_{\rm mb}$ is 1.03 ± 0.22 K, giving a velocity-integrated $T_{\rm mb}$ of $W({\rm CO(6-5)})$ ∼2.8 ± 0.5 K km s^{-1}. The corresponding integrated flux is $F({\rm CO(6-5)}) = 82.04$ Jy km s^{-1}, fainter than expected given $F({\rm CO(2-1)}) = 20.76 \pm 0.23$ Jy km s^{-1} (Öberg et al. 2011). For optically thick emission, if both lines stemmed from the same regions, the corresponding flux ratio $R_{21}^{65} = 3.95 \pm 0.70$ would require a common excitation temperature T = 14–20 K, given by the root of $R_{21}^{65} - B_{691.4}(T)/B_{230.5}(T)$. Öberg et al. (2011) report a major axis of 4.″6 ± 0.″2 in CO(2−1), in a solid angle of $\Omega_{\rm S} \sim 5.6\times10^{-10}$ sr. This indicates a representative temperature of $T \sim 19$ K, given by the root of $F({\rm CO(2-1)}) - \Omega_{\rm S}\sqrt{2\pi}B_{230.5}(T)\Delta_v^{21}/(2\sqrt{2\ln(2)})$, where $\Delta_v^{21} = 1.56$ km s^{-1} is the FWHM of CO(2−1). This representative temperature for the gas that originates CO(2−1) is close to the temperature for CO freezeout (≲19 K, e.g. Qi et al. 2011), and is also close to the highest temperatures allowed for CO(6−5), given the CHAMP+ data. Thus CO(6−5) is either less extended than CO(2−1), or it is modulated by a pointing offset. We caution that these integrated-flux data are affected by opposite biases from extended absorption in CO(2−1) and pointing offsets in CO(6−5).

[2] Consistent with a standard gas-to-dust ratio of 100 and a dust mass of ∼10^{-3} $M_\odot$ (Acke et al. 2004; Verhoeff et al. 2011).

3.2. Useful upper limits

3.2.1. CO(6–5)

VV Ser is coincident with extended CO(3–2) (COSURVEY), at $v_{\rm lsr} \sim 7$ km s^{-1}. Alonso-Albi et al. (2008) reported on interferometric continuum observations, and a CO(1–0) non-detection, interpreted as either an upper limit CO abundance of 2×10^{-6}, for a thin line, or beam-dilution of an optically thick line, with a representative CO disk radius $R_{\rm d} < 60$ AU for 200 K gas, and a distance of 260 pc. If optically thick, the CO(6–5) upper limit constrains the source solid angle to that of a disk with radius $R_{\rm d} < 0\farcs11(\Delta_v/3\ {\rm km\ s^1})^{-1/4}({\rm T_g}/50\ {\rm K})^{-1/2}$, at 3σ.

In *RX J1842.9-3532* a double-peaked Keplerian profile was found by Hughes et al. (2010) in CO(3–2), using the ASTE antenna. They find very low gas contents, which could result in optically thin CO(3–2) emission in parts of the disk. If optically thick, the CO(6–5) non-detection is probably due to beam dilution, with a solid angle ratio of less than 0.02 compared to CO(3–2). The CO(6–5) signal is unusually low given comparison data from the literature (see Sect. 4). Alternatively the CO(3–2) signal could be contaminated by extended CO, after all. We treat RX J1842.9-35 as an outlier, and avoid further discussion until higher-quality interferometric data are available.

HD 178253, alias α CrA, is located in the direction of the CrA molecular cloud (Harju et al. 1993), and shows bright CO(3–2) emission peaking at 0.6 K, as detected with the ASTE telescope (COSURVEY). However the CO(3–2) single-dish data shows strong contamination in the reference position, suggesting that most of the CO(3–2) emission stems from the CrA molecular cloud, although the presence of a weak underlying circumstellar component cannot be completely discarded. The CHAMP+ non-detection does not confirm the presence of warm circumstellar gas.

HD 37389 is located in the middle of Orion's belt, and is coincident with strong extended emission from Orion B, especially in the north-eastern horns of the CHAMP+ footprint. A single-pointing APEX CO(3–2) spectrum gives a narrow line, with a velocity-integrated $T_{\rm mb}$ flux of 4.2 K km s^{-1} (COSURVEY).

3.2.2. Non-detections of [C I](2–1)

Given that the critical density of [C II](2–1) is 930 cm^{-3} in a neutral medium, any [C I](2–1) emerging from a depth of ~100 AU would correspond to a total H I-nucleus column $N_{\rm H} < 1.5 \times 10^{18}$ cm^{-2}, which is much less than the $N_{\rm H} \sim 10^{21}$ cm^{-2} required for unit opacity in [C I](2–1). For an optically thin line, the mass of C in the excited state that falls in the telescope beam $\Omega_{\rm B}$ is $M({\rm C}(^3{\rm P}_2)) = m_{\rm C} D^2 \Omega_{\rm B} 4\pi F_\circ/(A_{21} h\nu)$, where $m_{\rm C}$ is the species' mass, $F_\circ$ is the observed frequency-integrated line flux, at frequency ν, and with decay rate A_{21}.

In the case of HD 142527, the frequency-integrated line flux for [C I](2–1) is <1.0 K km s^{-1}, at 3σ, and for a FWHM of 2.52 km s^{-1}. Correspondingly, $M({\rm C}(^3{\rm P}_2)) < 3.5 \times 10^{-8}\ M_\odot$ at 3σ. At $T_{\rm g} = 50$ K, the total C I mass is $M_{\rm C} < 1.1 \times 10^{-7}\ M_\odot$ for a two-level atom (and $<6.3 \times 10^{-8}\ M_\odot$ as $T_{\rm g} \to \infty$). For a total disk mass of ~0.1 $M\odot$, this upper limit $M_{\rm C}$ corresponds to an abundance of neutral C in rarefied gas (<10^3 cm^{-3}), relative to C in all forms[3], of less than 3.5×10^{-3}.

The [C I] flux limits in HD 142527 discriminates some of the disk models in Jonkheid et al. (2007, their model parameters are close to the case of HD 142527). Specifically, their models BL3 and BL4 have C I/C$^+$ ~ 10^{-2} at the disk surfaces (the highest points above the midplane in their Fig. 7). Models BL3 and BL4 correspond to depletions of small interstellar sized grains. Models B1, B4 and BL1 predict [C I] line fluxes $\lesssim$2 K km s^{-1} that could be compatible with the observed limit (their other models give [C I] line fluxes in the range 6–20 K km s^{-1}).

Previous searches for the C I content of HAeBe disks have also led to upper limits that motivate a comparison with model disks. In particular Chapillon et al. (2010) observed CQ Tau with an rms $T_{\rm A}^\star$ of 0.046 K for [C I](2–1), in 0.95 km s^{-1} channels; this is a factor of 3–5 deeper than values inferred from Table 1, corresponding to improved weather conditions (pwv < 0.3 mm). Chapillon et al. (2010) interpret their non-detections in terms of low gas-to-dust ratios: both their models and those by Jonkheid et al. (2007) predict significant C I signals for normal gas-to-dust ratios. In another recent C I search, Panić et al. (2010) invoke excess far-UV, and concomitant C$^+$ enrichment, to explain the factor of 10 discrepancy with predicted [C I] signals in HD 100546 (from models by Jonkheid et al. 2007, that otherwise match the rest of their data).

4. Discussion and conclusion

This CHAMP+ run resulted in a new southern disk with CO(6–5) emission, HD 142527. By contrast to CO(3–2), in HD 142527 the single-dish CO(6–5) is clear of contamination from extended emission. Higher-J CO lines are more robust for the single-dish identification of gas-rich systems: 4 out of 5 of the preliminary CO(3–2) measurements turned out to be extended emission (presumably from an ambient cloud). This is probably because the level population in $J = 6$ is lower in the diffuse ISM gas, or because of the finer beam size at the higher frequency.

Comparison with lower-J CO lines shows that in HD 142527 the CO(6–5) to CO(2–1) flux ratio is rather low, $R_{21}^{65} = 3.95 \pm 0.70$. Similar information is available in the literature for other sources with CO(6–5) detections. For LkCa 15 (K5V), the data in van Zadelhoff et al. (2001) give a flux ratio $R_{32}^{65} = 1.69 \pm 0.23$ (assigning 10% errors in the quoted $\int T_{\rm mb} {\rm d}v$), which would corresponding to an isothermal CO ladder at 12 K (for a common solid angle). However, these hints for rather low CO(6–5) fluxes are not systematic. All remaining sources in the literature have higher R_{32}^{65}, independent of spectral type. From Panić et al. (2010), in HD 100546 (B9V), $R_{32}^{65} = 4.42 \pm 0.70$ is consistent with the values of 3.3–4.0 corresponding to >50 K gas. Likewise, from Thi et al. (2001), in GM Aur (K5V), $R_{32}^{65} = 20.0 \pm 2.8$, in V892 Tau (B8), $R_{32}^{65} = 23.8 \pm 3.4$, in GG Tau (K6 V), $R_{32}^{65} = 6.5 \pm 0.9$, and in MWC 480 (A3V), $R_{32}^{65} = 8.1 \pm 1.2$. This apparent lack of correlation of R_{32}^{65} with spectral type may perhaps hint at the existence of an additional heating source other than starlight. A larger sample is required to draw statistically significant conclusions.

The [C I](2–1) observations resulted in new upper limits. The limit in HD 142527 constrains the fraction of carbon in low-density (<10^3 cm^{-3}) atomic gas to $<4\times10^{-3}$ (3σ). This limit also restricts the parameter space in the Ae stars models by (Jonkheid et al. 2007). Their models with gas-to-dust ratios greater or equal to 10^3 can be ruled out. Among models with normal dust abundance, those with total disk mass of 0.1 $M_\odot$ and 10^{-4} $M_\odot$ are compatible with the observed upper limit.

[3] For a cosmic carbon abundance of 3×10^{-4}.

Acknowledgements. We thank the referee for a thorough review with constructive comments that improved this research note. S.C., A.H., B.D., & F.M. acknowledge support from the Millennium Science Initiative (Chilean Ministry of Economy), through grant "Nucleus P10-022-F". S.C. acknowledges support from a Marie Curie International Incoming Fellowship (REA-236176), from FONDECYT grant 1100221, and the CATA ("Fondo Basal PFB-06, CONICYT"). I.d.G. acknowledges partial support from Ministerio de Ciencia e Innovacion (Spain), grant AYA2008-06189-C03-01.

References

Acke, B., van den Ancker, M. E., Dullemond, C. P., van Boekel, R., & Waters, L. B. F. M. 2004, A&A, 422, 621
Alexander, R. D., & Armitage, P. J. 2007, MNRAS, 375, 500
Alonso-Albi, T., Fuente, A., Bachiller, R., et al. 2008, ApJ, 680, 1289
Brinch, C., & Hogerheijde, M. R. 2010, A&A, 523, A25
Carmona, A. 2010, Earth Moon and Planets, 106, 71
Casassus, S., van der Plas, G., M, S. P., et al. 2013, Nature, 493, 191
Chapillon, E., Parise, B., Guilloteau, S., Dutrey, A., & Wakelam, V. 2010, A&A, 520, A61
Dent, W. R. F., Greaves, J. S., & Coulson, I. M. 2005, MNRAS, 359, 663
Dunkin, S. K., Barlow, M. J., & Ryan, S. G. 1997, MNRAS, 290, 165
Dutrey, A., Guilloteau, S., Duvert, G., et al. 1996, A&A, 309, 493
Duvert, G., Guilloteau, S., Ménard, F., Simon, M., & Dutrey, A. 2000, A&A, 355, 165
Fujiwara, H., Honda, M., Kataza, H., et al. 2006, ApJ, 644, L133
Fukagawa, M., Tamura, M., Itoh, Y., et al. 2006, ApJ, 636, L153
Fukagawa, M., Tamura, M., Itoh, Y., et al. 2010, PASJ, 62, 347
Güsten, R., Nyman, L. Å., Schilke, P., et al. 2006, A&A, 454, L13
Güsten, R., Baryshev, A., Bell, A., et al. 2008, in SPIE Conf., 7020
Harju, J., Haikala, L. K., Mattila, K., et al. 1993, A&A, 278, 569
Hughes, A. M., Wilner, D. J., Qi, C., & Hogerheijde, M. R. 2008, ApJ, 678, 1119
Hughes, A. M., Andrews, S. M., Wilner, D. J., et al. 2010, AJ, 140, 887
Jonkheid, B., Dullemond, C. P., Hogerheijde, M. R., & van Dishoeck, E. F. 2007, A&A, 463, 203
Malfait, K., Bogaert, E., & Waelkens, C. 1998, A&A, 331, 211
Menten, K. M., Wyrowski, F., Belloche, A., et al. 2011, A&A, 525, A77
Öberg, K. I., Qi, C., Fogel, J. K. J., et al. 2010, ApJ, 720, 480
Öberg, K. I., Qi, C., Fogel, J. K. J., et al. 2011, ApJ, 734, 98
Ohashi, N. 2008, Ap&SS, 313, 101
Panić, O., van Dishoeck, E. F., Hogerheijde, M. R., et al. 2010, A&A, 519, A110
Qi, C., Wilner, D. J., Calvet, N., et al. 2006, ApJ, 636, L157
Qi, C., D'Alessio, P., Öberg, K. I., et al. 2011, ApJ, 740, 84
Thi, W. F., van Dishoeck, E. F., Blake, G. A., et al. 2001, ApJ, 561, 1074
van Boekel, R., Min, M., Leinert, C., et al. 2004, Nature, 432, 479
Van Zadelhoff, G.-J., van Dishoeck, E. F., Thi, W.-F., & Blake, G. A. 2001, A&A, 377, 566
Verhoeff, A. P., Min, M., Pantin, E., et al. 2011, A&A, 528, A91
Wolf, S., & D'Angelo, G. 2005, ApJ, 619, 1114
Wootten, A., & Thompson, A. R. 2009, IEEE Proc., 97, 1463
Zuckerman, B., Forveille, T., & Kastner, J. H. 1995, Nature, 373, 494